

A new species of cryptic cyanobacteria isolated from the epidermis of a bottlenose dolphin and as a bioaerosol

Amber O. Brown, Caitlin S. Romanis, Petr Dvořák, Amanda J. Foss, Quincy A. Gibson, Chelsea D. Villanueva, Wendy N. Durden, Alyssa D. Garvey, Phillip Jenkins, Petr Hašler, Jeffrey R. Johansen, Brett A. Neilan & Dale A. Casamatta

To cite this article: Amber O. Brown, Caitlin S. Romanis, Petr Dvořák, Amanda J. Foss, Quincy A. Gibson, Chelsea D. Villanueva, Wendy N. Durden, Alyssa D. Garvey, Phillip Jenkins, Petr Hašler, Jeffrey R. Johansen, Brett A. Neilan & Dale A. Casamatta (2021): A new species of cryptic cyanobacteria isolated from the epidermis of a bottlenose dolphin and as a bioaerosol, *Phycologia*, DOI: [10.1080/00318884.2021.1968173](https://doi.org/10.1080/00318884.2021.1968173)

To link to this article: <https://doi.org/10.1080/00318884.2021.1968173>



View supplementary material [↗](#)



Published online: 29 Sep 2021.



Submit your article to this journal [↗](#)



View related articles [↗](#)



View Crossmark data [↗](#)



A new species of cryptic cyanobacteria isolated from the epidermis of a bottlenose dolphin and as a bioaerosol

AMBER O. BROWN ^{1,2}, CAITLIN S. ROMANIS ³, PETR DVOŘÁK ⁴, AMANDA J. FOSS ⁵, QUINCY A. GIBSON ⁶,
CHELSEA D. VILLANUEVA ⁷, WENDY N. DURDEN ⁸, ALYSSA D. GARVEY⁵, PHILLIP JENKINS⁹, PETR HAŠLER ⁴, JEFFREY R. JOHANSEN ^{10,11},
BRETT A. NEILAN ³ AND DALE A. CASAMATTA ⁶

¹School of Mathematical and Physical Sciences, University of Technology Sydney, 15 Broadway, Ultimo, NSW 2007, Australia

²Australian Museum, Australian Museum Research Institute, Sydney, NSW 2001, Australia

³School of Environmental and Life Sciences, University of Newcastle, University Drive, Callaghan, NSW 2308, Australia

⁴Department of Botany, Faculty of Science, Palacký University Olomouc Šlechtitelů 27, Olomouc, 783 71, Czech Republic

⁵Greenwater Laboratories, 205 Zeagler Dr, Palatka, Florida 32177, USA

⁶Department of Biology, University of North Florida, 1 University of North Florida Drive, Jacksonville, Florida 32224, USA

⁷Department of Biological, Geological, & Environmental Sciences, Cleveland State University, 2121 Euclid Avenue, Cleveland, Ohio 44115, USA

⁸Hubbs-SeaWorld Research Institute, 3830 South Highway A1A #4-181, Melbourne Beach, Florida 32951, USA

⁹College of Medicine, University of Florida, 1600 SW Archer Rd M509, Gainesville, Florida 32610, USA

¹⁰Department of Biology, John Carroll University, 1 John Carroll Blvd., University Heights, Ohio 44118, USA

¹¹Department of Botany Faculty of Sciences, University of South Bohemia, Branišovská 31, České Budějovice 370 05, Czechia

ABSTRACT

Two cyanobacterial strains, one collected from an epidermal mat present on a dead bottlenose dolphin and the other as a bioaerosol 457 m (1500 ft) above the river, were recently analysed from the St. Johns River, Jacksonville, Florida, USA. Both samples had major phenotypic plasticity which confused morphological identification. Amplicon sequencing of the 16S rRNA gene from the isolates revealed that both samples were closely aligned (branch bootstrap support = 100%) with the recently erected genus *Komarekiella*. Whole genome sequencing and phylogenetic construction also supported the isolation of a new species of cyanobacteria branching from the *Nostoc* clade. A total evidence approach of molecular, genetic, and ecological examination of these strains supported the erection of a new species, *Komarekiella delphini-convector*. A prior study determined that the dolphin with the epidermal mat had low levels of microcystins/nodularins (MCs/NODs) in the hepatic tissue. To investigate whether these toxins originated from the epidermal mat, immunoassay (ELISA) and 2-methyl-3-methoxy-4-phenylbutyric acid (MMPB) techniques were conducted on the original mat and subsequent culture samples. The results from both analyses were not conclusive. Genome mining was conducted and revealed diverse biosynthetic capabilities of this species but could not support toxin-producing potential. Further analytical work is required to determine the pathogenic capacity of this epizotic species.

ARTICLE HISTORY

Received 14 April 2021
Accepted 11 August 2021
Published online 29
September 2021

KEYWORDS

16S-ITS-23S rDNA; Genome mining; Secondary metabolites; *Tursiops truncatus*

INTRODUCTION

Cyanobacteria are a ubiquitous collection of oxy-photosynthetic prokaryotes with diverse ecologies and sometimes cryptic morphologies that often complicate species identification. Accurate species-level determination of cyanobacteria is critical for many theoretical and practical aspects, including studies of biogeography, ecosystem health and water quality (Douterelo *et al.* 2004; Wehr *et al.* 2015). Ecosystem, human and animal health assessments also rely on correct species identification, as some cyanobacterial species produce toxic secondary metabolites (cyanotoxins) while other morphologically similar species or strains are nontoxic (Otsuka *et al.* 1999; Laamanen *et al.* 2001; Christiansen *et al.* 2008).

Elucidating cyanobacterial species identity through morphological analysis is complicated by phenotypic plasticity of many taxa, allowing for various morphotypes within a species

(Casamatta *et al.* 2003; Dvořák *et al.* 2014; Komárek *et al.* 2014). The challenges in cyanobacterial systematics have been addressed with polyphasic approaches that have combined morphological, genetic and ecological methods to aid classification (Komárek 2003, 2010; Komárek *et al.* 2014; Johansen & Casamatta 2005). However, due to the assortment of methods employed, some previously recognized cyanobacterial lineages are now known to be polyphyletic and significant revision is needed to reach classifications with only monophyletic groups (Komárek 2003; Johansen & Casamatta 2005; Dvořák *et al.* 2014). Modern species assignment utilizes 16S rDNA-based phylogeny with corresponding analysis of secondary structure, produced by the folding of the highly conserved domains within the 16S-23S Internal Transcribed Spacer (ITS) region (Iteman *et al.* 2000; Boyer *et al.* 2001; Johansen & Casamatta 2005). Sometimes, these methods are unable to delineate species with

various ecotypes, or species that have undergone significant convergent events (Dvořák *et al.* 2014). Instead, species with complex evolutionary and ecological histories require multi-loci and whole genome analyses for evolutionary and phylogenetic clarification (Dvořák *et al.* 2014). Furthermore, whole genome sequencing of cyanobacteria is beneficial in providing supplementary information, including determining the potential for toxic secondary metabolite production.

Bottlenose dolphins (*Tursiops truncatus* Montagu 1821) have been recently described to be negatively impacted by toxigenic cyanobacteria (Brown *et al.* 2018). Both coastal and estuarine dolphins are exposed to a variety of cyanotoxins (Brown *et al.* 2018; Davis *et al.* 2019), indicating that the impacts of these toxins are far reaching. Additionally, both live and deceased dolphins have been documented to have non-descript 'algal sheens' and 'epidermal algal mats' in the southeastern United States (e.g. Jacksonville, Florida; Ormond Beach, Florida; Lake Pontchartrain, Louisiana) (Florida Fish and Wildlife Conservation Commission and Wildlife Research Institute – FWC-FWRI, unpublished data; W.N. Durden, unpublished data; Barry *et al.* 2008; Mullin *et al.* 2015). The presence of epidermal-type microbial aggregations was also reported as a clinical feature across a number of stranded dolphins in the 2019 unusual mortality event (UME) in the Northern Gulf of Mexico (NOAA 2019). Epidermal-type growths are typically associated with dolphins that are inhabiting or are exposed to freshwater (Barry *et al.* 2008; W.N. Durden, unpublished data; Q.A. Gibson, unpublished data), either due to large freshwater discharge events (e.g. unusual weather events, dam releases) or from the straying out of their normal habitats (Barry *et al.* 2008; Carmichael *et al.* 2012; Ewing *et al.* 2017). Low salinity exposure, regardless of duration, has been shown to significantly alter the physiology of dolphins (Ewing *et al.* 2017), leading to depressed immune systems, skin lesions and mortalities (Wilson *et al.* 1999; Carmichael *et al.* 2012). It is also suspected that skin lesions have facilitated opportunistic infections and epidermal growths (Wilson *et al.* 1999; Barry *et al.* 2008; Mullin *et al.* 2015). However, to date, there have been no published reports to articulate the species identities of these epidermal microbial constituents or their potential to affect marine mammal health. As a result, the potential impacts that microbial mat species have had on dolphin and ecosystem health is unknown. It is critical to identify these potential relationships to adequately assess the impacts that epidermal microbial mats may have on dolphin health for future preventative and reactive management (e.g. rescue and rehabilitation) strategies.

The St Johns River (SJR; Jacksonville, Florida) is a large, brackish, estuarine system that provides a critical habitat for a genetically and behaviourally distinct community of bottlenose dolphins (Caldwell 2001; Gubbins 2002; Ermak *et al.* 2017). This community is routinely surveyed in low salinity (0–18 ppt) habitats (Caldwell 2001; Gubbins 2002; Ermak *et al.* 2017). These dolphins have been subjected to widespread health decline (i.e. emaciation, skin lesions, cyanotoxin exposure; Brown *et al.* 2018; Q.A. Gibson, unpublished data) and two UMEs since 2010 (Environmental Protection Board

2017). Additionally, between 2008 and 2015, three dolphins were discovered (attempted rescue; TtNEFL0813, or recovered dead; TtNEFL1501, TtNEFL1511) with thick epidermal mats of unknown composition (FWC-FWRI, unpublished data).

In November 2016, an investigation into the cryo-archived epidermal mat of TtNEFL1501 was conducted after the detection of cyanotoxins, microcystins/nodularins (MCs/NODs), in the dolphin's hepatic tissue (Brown *et al.* 2018). Both the preliminary microscopic examination and the subsequent culture of the mat revealed the presence of cyanobacteria. However, species identification could not be immediately confirmed, as the cultures contained various morphotypes. Additionally, in an unrelated sampling event that occurred over the SJR in July 2017, a cyanobacterial strain was collected at 457 m that had similar displays of various morphotypes in culture.

The objectives of this research were to identify the species, as well as the capacity to produce toxic secondary metabolites, of the polymorphic cyanobacterial strains collected. Genetic methodologies (whole genome assessment and 16S rDNA phylogeny) were combined with morphologic and ecological analysis to classify the cyanobacteria. Additional toxicological (ELISA, MMPB, genome mining) analyses were conducted to determine the toxin-producing capabilities of this species. Evidence obtained through this polyphasic approach supports the erection of a new species within the genus *Komarekiella*, which we name *Komarekiella delphini-convector* sp. nov.

MATERIAL AND METHODS

Epidermal mat sample collection and dorsal fin identification

The cryo-archived epidermal mat sample, necropsy report, necropsy photographs and GPS coordinates of stranding location for TtNEFL1501 were provided by FWC-FWRI under permission from NOAA's Code of Federal Regulations 50CFR216.22. TtNEFL1501 was an adult male (271 cm total length) recovered on 17 January 2015 from an oligohaline habitat in Green Cove Springs, Florida (30°1.745'N, 81°41.764'W). This dolphin was identified as a known member of the SJR estuarine population (MKNA) through the UNF photo-identification catalogue by comparing distinctive dorsal fin features (i.e. nick and notch patterns, fin shape) from photographs taken during necropsy to those taken during behavioural surveys. Two epidermal algal mat samples (0.05 g and 0.06 g wet weight) were excised during routine necropsy and stored at –20°C in a sterile Whirl-pak® until culture.

Air sample collection

A Microbial Aerial Sampling Kit (MASK; Fig. S1) was built for the sterile collection of aerosolized samples from the window of an aircraft. Falcon tubes with perforated bottoms were filled with dry, sterile cotton and autoclaved. Prior to and between deployments, the MASK was sterilized with 95% ethanol. After receiving the required approval, a Cessna 172

Skyhawk was contracted for air sampling. Samples were collected over the St. Johns River (30°7.1502'N, 81°40.4214'W) at c. 457 m (1500 ft), 914 m (3000 ft) and 1372 m (4500 ft). Circular transects at each altitude were marked by coordinates using JEVAG waypoint: OpenNav aviation database. After sampling, cartridges were transferred to individual Whirlpaks® for transportation.

Isolation of cyanobacteria into culture

A small subsample of the cryo-archived epidermal mat sample was removed and initially plated on solidified BG-11 (Allen & Stanier 1968) and solidified Z-8 (Staub 1961) media until enough growth was achieved for sub-culturing. Samples collected using the MASK were cultured through direct inoculation of cotton onto sterile Z-8 medium. Subcultures of both dolphin epidermal mat and air sample cultures were then isolated using standard isolation techniques (Andersen 2005), plated on nitrogen-free BG-11 and Z-8 media (Staub 1961), and grown for two months. Subcultures were continuously sampled and isolated until unialgal growth was achieved.

Microscopic identification and morphological analyses

Samples from the BG-11 and Z-8 dolphin epidermal mat cultures were prepared and photographed using a Zeiss AxioImager microscope (objective α -Plan-Apochromat 100 \times , oil, DIC, N. A. = 1.46) with a Zeiss AxioCam D512 camera (Carl Zeiss AG, Oberkochen, Germany) (12 MPx). Photos were taken and processed using Zeiss AxioVision software (ver. 4.9.1).

DNA extraction and cloning

DNA from both dolphin epidermal mat subcultures and air sample subcultures were extracted using the PowerSoil™ DNA Kit (Mo Bio Laboratories Inc., Carlsbad, California, USA) with 0.25 g of cultured sample and checked on an ethidium bromide stained 1.5% agarose gel. PCR amplification of the partial 16S rRNA gene was performed using primers forward 8 F and reverse B23S (Lane 1991). The ITS PCR amplification was performed using primers forward VRF5 and reverse VRF1 (Boyer et al. 2001). The PCR amplification was conducted at a final volume of 50 μ l, containing 19 μ l sterile water, 2 μ l of each primer (0.01 mM final concentration), 25 μ l PCR Master Mix (Promega, Madison, WI) and 2 μ l template DNA (50 ng μ l⁻¹), following parameters outlined in Casamatta et al. (2003). Both amplified 16S and ITS DNA were cloned into pGEM® T Vector System I and JM-109 High Efficiency Competent Cells (Promega, Madison, Wisconsin, USA) that were cultured using carbenicillin-infused LB media. Plasmid DNA was purified from eight replicate, transformed competent colonies per isolate, using QIAprep® Spin Miniprep Kits (QIAGEN, Hilden, Germany). Sequencing of cDNA libraries was performed by Eurofins Genomics (MWG Operon Inc., Louisville, Kentucky, USA).

Whole genome sequencing

The culture produced by the dolphin epidermal mat sample was selected for whole genome sequencing. The sequencing library

was prepared by Nextera DNA Library Preparation Kit (Illumina Inc., San Diego, California, USA) using 50 ng of DNA. Fragment length selection was performed by Agilent High Sensitivity DNA Kit (Agilent Technologies, Inc., Santa Clara, California, USA) (insert size 1000 bp). The library concentration was evaluated by KAPA Library Quantification Kit for Illumina (Kapa Biosystems, Woburn, Massachusetts, USA). Sequencing was performed on an Illumina MiSeq platform for 300 bp \times 2 paired end reads using the V3 kit at the Institute of Experimental Botany of Czech Academy of Sciences (Olomouc, Czech Republic).

Prior to assembly, quality assessment of the reads was performed using Trimmomatic 0.36 (Bolger et al. 2014). Adapters were removed and a sliding window approach was taken to excise bases with an average quality lower than 15. Reads shorter than 50 bp were removed. Filtered reads were assembled using Spades 3.10.1 (Bankevich et al. 2012) with default settings. Produced scaffolds were binned by Maxbin 2.2.4 (Wu et al. 2016) to remove contaminant bacterial genomes. The *Komarekiella* genome was annotated using the RASTtk annotation scheme (Aziz et al. 2008).

Specialized secondary metabolite biosynthetic gene cluster detection

Secondary metabolite biosynthetic gene clusters (smBCGs) in the *Komarekiella delphini-convector* genome produced from the dolphin epidermal mat subculture were identified using antiSMASH (Blin et al. 2019), BAGEL4 (Van Heel et al. 2018), NaPDoS (Ziemert et al. 2012) and PRISM (Skinnider et al. 2015). Any smBCGs that were predicted to be involved in the synthesis of microcystin or nodularin were further examined using BLASTn and BLASTp to confirm their putative gene function.

16S rDNA phylogenetic analyses

Two-hundred and forty-eight cyanobacterial 16S rDNA sequences were retrieved from the NCBI nucleotide database (<https://www.ncbi.nlm.nih.gov/nucleotide/>) and combined with the 16S rDNA sequences produced from the dolphin epidermal mat and the air sample subcultures for phylogenetic analysis. In instances where a cyanobacterial RefSeq genome was available, the 16S rDNA was extracted using RNAmmer version 1.2 (Lagesen et al. 2007). Sequences were aligned using MUSCLE (Edgar 2004) and manually optimized by removing truncated sequences and eliminating nonhomologous regions. The appropriate nucleotide substitution model for phylogeny construction for both Maximum Likelihood and Bayesian Inference was determined to be GTR+I+G using jModelTest2 version 2.1.10 (Darriba et al. 2012). Maximum Likelihood (ML) phylogenetic analysis was performed by RaxML v.8 (Stamatakis 2003) using the automatic bootstrapping criterion autoMRE. Bayesian Inference calculations were run in MrBayes 3.2.7a (Ronquist et al. 2012). The Markov Chain Monte Carlo (MCMC) inference was calculated for 700,000,000 generations. The convergence criterion reached a value <0.01. The final trees were annotated using

the Interactive Tree of Life (iTOL) v4 (Letunic & Bork 2019) where nodes with bootstrap values <30 were collapsed.

Phylogenomic analyses

The reference cyanobacterial genomes were downloaded from NCBI ftp server (ftp://ftp.ncbi.nlm.nih.gov/genbank; Table S1). An orthologous single-copy genes group selection was performed in Hal (Robbertse *et al.* 2011); each set of orthologs must have been 80% complete. Using these parameters, 846 groups were retrieved. Subsequent orthologous gene groups were aligned using MUSCLE 3.6 (Edgar 2004) and filtered by Gblocks 0.91 (Castresana 2000) with option - b5 = h. The ML phylogenetic reconstruction was performed in IQ-TREE 1.6.5 (Nguyen *et al.* 2015). The best model was identified based on BIC - cpREV + F + I + G4 and the tree topology was tested by ultrafast bootstrap re-samplings with 2000 replicates.

16S-ITS-23S secondary structure analyses

The secondary structures of the following conserved domains (D1-D1', Box-B, V2 and the V3 helices) of 16S-ITS-23S region were comparatively analysed for both cultured isolates. The secondary structures of ITS motifs for both strains and closely related taxa were qualitatively compared through predicted RNA folding using the untangle loop fix structure draw mode in Mfold (Zuker 2003). The domain lengths of the full ITS sequences were measured, and p-distances were calculated and compared to closely related taxa.

The secondary structure estimations were made following the models for the 16S rRNA, 23S rRNA and 5S rRNA regions published for *Scytonema hyalinum* N.L. Gardner (Johansen *et al.* 2017). Modifications for longer or shorter helices were required for selected helices, and the terminal structures of the helices were determined in Mfold 3.2 (Zuker 2003). The secondary structure figures were then manually assembled in Adobe Illustrator CS5 version 15.0.0.

Toxin analyses: free Adda microcystins/nodularins (MCs/NODs)

Cultured isolates from the dolphin epidermal sample and the original epidermal mat sample were homogenized and extracted for free Adda microcystins and nodularins (MCs/NODs). Cyanobacterial growth was removed from the agar of both BG-11 and Z-8 dolphin epidermal culture samples using a sterile razor blade. Each culture (*c.* 500 mg) and the mat sample (54 mg) were placed in 7 ml homogenization tubes containing 2.3 g stainless steel beads (2.4 mm). Buffer (10 mM phosphate buffer; pH = 7) was added to bring samples to 250 mg ml⁻¹ (cultures) and 50 mg ml⁻¹ (mat) sample concentrations and homogenized (5.5 m s⁻¹ for 15 s) via a bead Rupter 24 (Omni Kennesaw, Georgia, USA). Aliquots were removed corresponding to 50 mg material (200 µl of cultures and of entire mat sample), with duplicates of cultured samples spiked at 20 ng g⁻¹ using certified reference material (CRM) of MC-LR (National Research Council of Canada, Halifax, Nova Scotia, Canada).

Extraction was conducted by adding 5 ml of extraction solution (75% MeOH in 100 mM acetic acid) followed with vortex mixing and bath sonication (25 min). Samples were centrifuged (10 min; 1500× *g*), supernatants retained, and the pellet was rinsed with extraction solution via vortex mixing (1 ml). Solutions were re-centrifuged and resulting supernatants were combined, methanol was removed under a stream of N₂ at 60°C and extracts diluted (5 ml) in deionized water (DI). Samples were loaded onto 100 mg preconditioned (MeOH followed by DI) Strata-X solid phase extraction (SPE; Phenomenex, Torrance, California, USA), rinsed (2 ml DI) and eluted (3 ml 90% acetonitrile). Eluates were blown to dryness (60°C, N₂), reconstituted (0.5–1 ml DI) and filtered (0.2 µm polyvinylidene fluoride) prior to analysis.

A polyclonal Adda ELISA (Abraxis Kits, PN 520011, Warminster, Pennsylvania, USA) was used for free MCs/NODs analysis as described in Foss *et al.* (2017). Culture samples were analysed at a sample concentration of 50 mg ml⁻¹, resulting in a detection limit of 3 ng g⁻¹ (ppb) based on kit sensitivity (0.15 ng ml⁻¹) and sample dilution factor (DF = 20). The mat sample was analysed at 100 mg ml⁻¹, resulting in a detection limit of 1.5 ng g⁻¹ (ppb).

Toxin analyses: total Adda MCs/NODs oxidation (MMPB) and analysis

Extracts prepared for free MC/NOD analysis by Adda ELISA and previously unextracted original epidermal mat and epidermal mat cultured isolates were oxidized, extracted and analysed for MMPB. Duplicate subsets of culture material were spiked before oxidation at 2 and 5 ng g⁻¹ using a CRM of MC-LR. Oxidations were conducted as previously described (Brown *et al.* 2018). Briefly, extracts (100 µl) were oxidized for 30 min in 100 mM K₂CO₃, 15 mM KMnO₄, 15 mM NaIO₄, and unextracted samples (50 mg of mat sample; 250 mg of culture) were oxidized in 5 ml of 0.2 M K₂CO₃, 0.1 M KMnO₄, 0.1 M NaIO₄ solution for 2 h. Reactions were stopped via dropwise addition of 40% (w/v) sodium bisulphite. Solutions were applied to preconditioned (MeOH followed with DI) Strata X SPE (200 mg), rinsed (3 ml DI) and eluted (5 ml 90% ACN). The samples were blown to dryness (N₂ 60°C) and reconstituted in DI water. Previously extracted samples were reconstituted to achieve 50 mg ml⁻¹ (cultures) and 100 mg ml⁻¹ (mat). The remaining samples were reconstituted to achieve sample concentrations of 500 mg ml⁻¹ (cultures) and 50 mg ml⁻¹ (mat).

MMPB was analysed using liquid chromatography tandem mass spectrometry (LC-MS/MS) as described in Foss *et al.* (2017) using a Surveyor HPLC system coupled with a TSQ Triple Quadrupole Mass Spectrometer equipped with a Heated Electrospray Ionization (HESI-II) Probe (Thermo Scientific, Waltham, MA, USA). Compounds were separated using a Kinetex F5 column (2.6 µm; 100 Å; 150 × 2.1 mm; Phenomenex) running 0.2 mL min⁻¹ isocratically (60% methanol in 0.05% acetic acid). The MMPB [M-H]⁻ ion, (*m/z* 207), was fragmented (12% CE) and the product ion (*m/z* 131) was monitored. The method detection limit was determined using a signal to noise ratio of 3. External curves

generated of oxidized MC-LR in water (0.25, 0.5, 1, 5, 10 ng mL⁻¹) were used to determine spike recoveries.

Home range and core area determination

Weekly dolphin photo-identification surveys were conducted along a fixed 40-km transect described in Ermak *et al.* (2017). TtNEFL1501 had 20 sightings from 2011–2015 after same-day resights were removed. Sighting locations were plotted in ArcGIS 10.4.1 (ESRI; Redlands, California, USA) and were transformed into a univariate dataset. A midline was run through the middle of the survey route and downtown Jacksonville was designated as location 0 while the Mayport Inlet was designated as location 40. Sighting locations were transformed to the midline via the 'locate features along routes' tool. The generated univariate dataset was input into SAS (version 9.4; SAS Institute, Cary, North Carolina, USA) and the PROC KDE function was used to calculate 95% (home range) and 50% (core area) utilization distributions. To select bandwidth, the simple normal reference (SNR), Silverman's rule of thumb (SROT), and the Sheather-Jones plug in (SJPI) methodologies were compared. SROT was selected as the appropriate bandwidth as it moderately smoothed the data.

RESULTS

Description of a new taxon

Based on a total evidence approach of molecular, genetic and ecological characters, we propose *Komarekiella delphini-convector* as a new species under the International Code of Nomenclature for algae, fungi and plants (ICN; Turland *et al.* 2018).

***Komarekiella delphini-convector* A.O. Brown, P. Dvořák, Garvey, C.D. Villanueva & Casamatta sp. nov.**

Figs 1–15

DESCRIPTION: Colony spreading on agar, with filaments penetrating the agar when mature, microscopic to macroscopic both in culture and from original samples, sandy-brown in nature, then dark blue-green, later turning jade green in culture, consisting of subspherical colonies. Colonies initially consisting of aggregates of hormocytes, which later differentiate into filaments via cell division perpendicular to the filament axis. Filaments consist of uni- to multiseriate rows of cells, branching usually not present but occasional formation of uniseriate lateral branches observed. Sheath usually diffuent, homogenous and colourless, seldom delimited. Hormogonia frequently observed, small (*c.* 3 µm wide) and few-celled (3–8 cells per filament). Vegetative cells mainly spherical to barrel-shaped, 3–5 µm in diameter. Heterocytes intercalary, barrel-shaped, 3–6 µm in diameter. Akinetes spherical to oval, 6–10 × 6–12 µm, apoheterocytic, frequently forming multiseriate filaments when initiating cell division. Reproduction by disintegration of colonies and germination of akinetes into short hormogonia. GenBank accession numbers VJXY00000000 (whole genome of SJRDD-AB1); MN583267 (partial 16S rRNA gene + 16S-ITS-23S of SJR-PJCV1).

HOLOTYPE: OLM Botany 24: Lichens and others No. 9228, metabolically inactive, dried reference strain (SJRDD-AB1), deposited in the Regional Museum in Olomouc, Czech Republic.

PARATYPE: Herbarium material preserved by drying of the strain SJR-PJCV1.

AUTHENTIC STRAIN: (SJRDD-AB1) Culture collection of cyanobacteria and algae at the Department of Botany, Palacký University, Olomouc, Czech Republic, strain UPOC 179/2019.

TYPE LOCALITY: Epizoic on dead bottlenose dolphin, St. John's River, northeast Florida, 30°1.745'N, 81°41.764'W, collected 17 January 2015. Previous literature described *Komarekiella* as both an epiphyte and an epilith (Hentschke *et al.* 2017).

ETYMOLOGY: Latin *delphini-convector*, dolphin's travelling companion, in reference to the retrieval location of the holotype and reference strain.

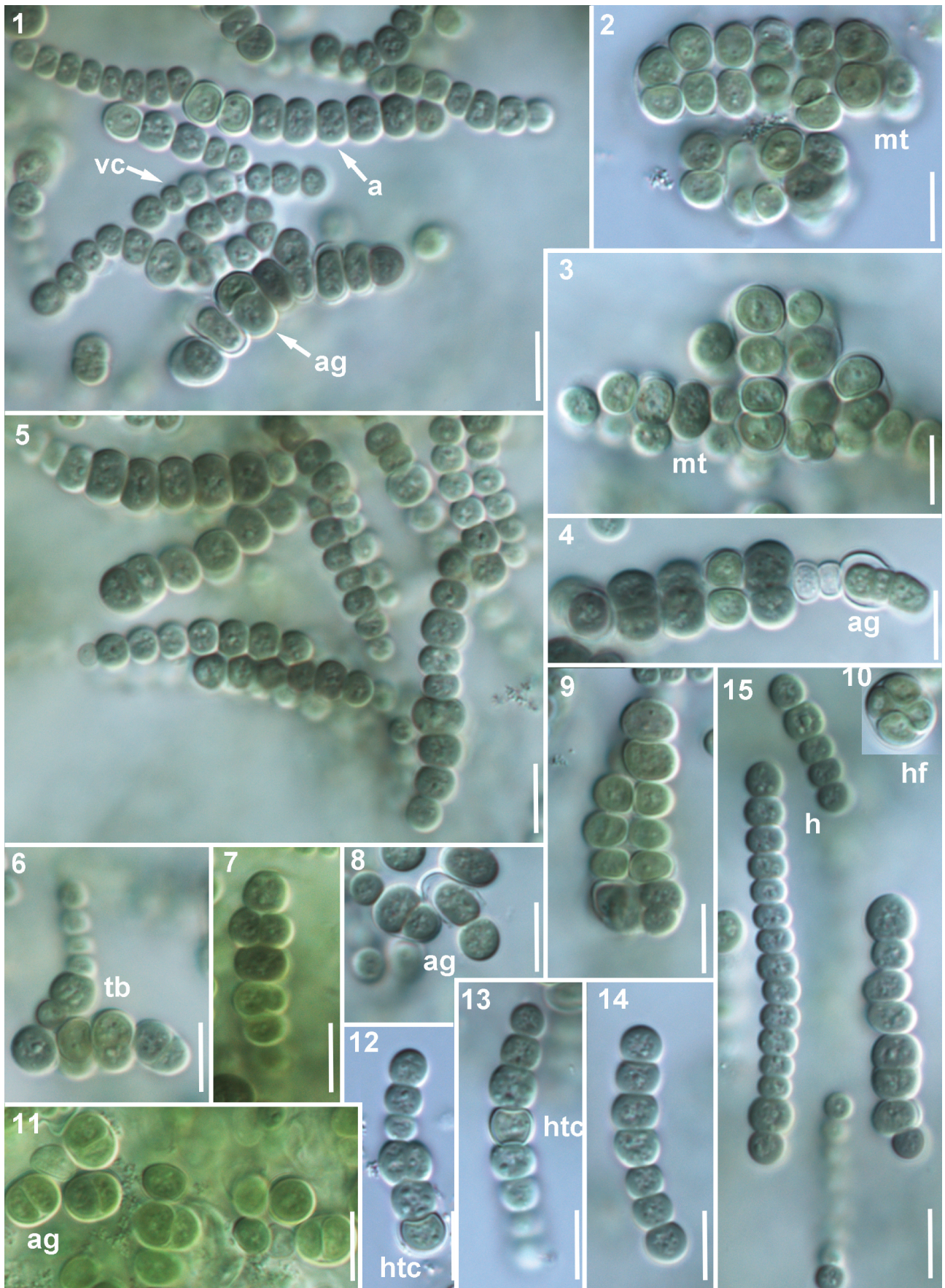
Morphology

The morphological descriptions were conducted on cultured specimens isolated from the dolphin epidermal mat. *Komarekiella delphini-convector* was morphologically similar to *Komarekiella atlantica* Hentschke, J.R. Johansen & Sant'Anna (Hentschke *et al.* 2017), exhibiting similar unusual features such as the capacity to undergo radical morphological changes. Hormogonia resembled fragments, as seen in some species of *Nostoc* (Bornet & Flahault 1886), and other cells congregated into pseudo-sarcinoid packets (Figs 1–3). *Komarekiella delphini-convector* had single cells that varied greatly in size and colour (Figs 1, 4, 11–12). Some stages of colonial development were morphologically similar to *Anabaena* (Fig. 15), while other cells resembled unicellular *Synechocystis*, or appeared as aggregates of filamentous and/or packet-like cells typically associated with Chlorogloeopsidaceae. Filaments were either uni- or multi-seriate (Figs 5, 7, 9) with a mixture of both structures found within the same culture. Unlike *Chlorogloeopsis* A.K. Mitra & D. C. Pandey and *Komarekiella atlantica*, *K. delphini-convector* had heterocytes that were both similar in size, and at times larger than, vegetative cells (Figs 12–14). As in the type species of *Komarekiella*, *K. atlantica*, akinetes of *K. delphini-convector* developed apoheterocytically and subsequently formed multiseriate filaments or short hormogonia (Figs 7, 10). On the other hand, akinetes of *K. delphini-convector* are spherical to oval (Figs 1, 4, 8), and larger than those of *K. atlantica*. Additionally, true branching was present in *K. delphini-convector* (Fig. 6).

Genome annotation and genome mining

The final assembled *K. delphini-convector* draft genome was 8.5 Mbp, with 174 scaffolds, a N50 value of 127Kb and 97.2% predicted completeness. The GC content of the genome was 41.4% and the genome annotation revealed 8714 coding sequences (3168 genes were hypothetical) and 47 RNAs (Fig. 16).

Prediction of secondary metabolite biosynthetic gene clusters (smBGCs) was conducted using NaPDoS, antiSMASH, BAGEL4 and PRISM (Table S2). NaPDoS identified 30 condensation (C) domains and 18 ketosynthase (K) domains. Of these, nine domains were predicted to be involved in the synthesis of microcystin with 49%–58% similarity to characterized pathways. NaPDoS identified 30 condensation (C) domains and 18 ketosynthase (K) domains. Six of these condensation domains had low similarity predictions to microcystin synthesis based on similarities to previously characterized pathways; NODE27: 40–341 bp 51%, NODE38: 2442–2749 bp 55%, NODE67: 141–



444 bp 58%, NODE482: 141–445 bp 56%, NODE38: 22–325 bp 56%, NODE341: 1–213 bp 55%. Interestingly, three domains had high similarity (57%–100%) to characterized anabaenopeptin/nostamide pathways (Table S2). PRISM identified 16 clusters associated with specialized metabolite production; four non-ribosomal peptide synthetase (NRPS), three polyketide synthase (PKS), six NRPS-PKS clusters as well as two lassopeptide clusters and one microviridin. Of the NRPS clusters, two putative microcystin smBGCs (NODE482: 141–445 bp and NODE341: 1–213 bp) were predicted. Conversely, antiSMASH only recognized similarity between known microcystin biosynthetic pathways and NODE341: 1–213 bp (30%). A single NRPS domain was detected on NODE482: 141–445 bp by antiSMASH with a MIBiG *mcvB* annotation of (53%). BLASTp was used to confirm the gene composition of the microcystin-associated smBGCs where four nodes (NODE67: 141–444 bp, NODE38: 22–325 bp, NODE341: 1–213 bp and NODE482: 141–445 bp) were identified as containing the microcystin synthetase gene *mcvB* with 98%–100% query matching. While additional genes implicated in the synthesis of hepatotoxins were putatively annotated, such as *ndaA* and *crpD*, the remaining suite of *mcv* genes were not identified within any of the microcystin-associated smBGCs, limiting conclusions pertaining to microcystin synthesis by the novel *K. delphini-convector* species.

Phylogeny

Komarekiella delphini-convector was established as a new candidate species through phylogenetic assessment conducted using the 16S rDNA sequences of 248 cyanobacterial strains, including the two *K. delphini-convector* strains. In a Maximum Likelihood (ML) analysis the *K. delphini-convector* strains clustered with six *K. atlantica* strains (node bootstrap support = 30%) (Fig. 17). Furthermore, this branch of the phylogenetic tree is supported as a new species within the *Komarekiella* genus (branch bootstrap support = 88%). Within the *Komarekiella* clade, two *Nostoc* species were also present; *Nostoc* sp. CENA107 and *Nostoc* sp. 9E-03, suggesting that these strains were previously misidentified. *Nostoc* sp. 9E-03 was previously described to be within the same clade as *Nostoc* sp. CENA107 by Cuzman *et al.* (2010). This species was identified through 16S rDNA sequencing of photosynthetic biofilms in Monumental Fountains (Cuzman *et al.*

2010) while *Nostoc* sp. CENA107 was previously discovered when monitoring a wastewater stabilization pond (Furtado *et al.* 2009). This new analysis separates these as two distinct species, both belonging to the genus *Komarekiella*. The Bayesian analyses of the 16S rDNA sequences supported that *K. delphini-convector* is a new species with posterior probability support of 0.98 for the clade (Fig. 18). A similar genetic resemblance to *Nostoc* was observed in the phylogenomic ML tree where *K. delphini-convector* was placed in a clade containing *Nostoc* species with 100% ultra-fast bootstrap support (Fig. 19). However, this is likely either because *Komarekiella* was not yet an established genus when those species were identified, the full genome of *K. atlantica* has not been sequenced, or that the available *Nostoc* strains were misidentified.

Secondary structure analyses (16S-ITS-23S)

Comparisons of conserved ITS domain secondary structures showed distinct variations between the new taxon and available structures from the sister species *K. atlantica*. The D1-D1' helix for *K. delphini-convector* had a single nucleotide change, which altered the basal clamp from 4 bp to 5 bp, subsequently constricting the basal unilateral bulge (Fig. 20). Furthermore, the internal bilateral bulge, 5'-AA:A-3', is displaced 2 bp towards the apex in comparison to *K. atlantica* (Fig. 20, diagrams B–D). The sister genera were all distinctly different in the structure of the D1-D1' helix in comparison to both *Komarekiella* species (Fig. 20). Analyses of the Box-B helix revealed a 2-bp insert centred between the internal bilateral and terminal loop, as well as two nucleotide substitutions in the terminal loop (not affecting structure) in *K. delphini-convector* as compared to *K. atlantica* (Fig. 21). *Komarekiella atlantica* Box-B helices were identical among strains and shared the same sequence in the basal bilateral bulge (Fig. 21). Sister genera showed considerably greater divergence in structure in comparison to the *Komarekiella* species (Fig. 21).

The V2 helices, situated between the tRNA^{Ile} and tRNA^{Ala} genes, were similar in both *Komarekiella* species (Fig. 22), although *K. atlantica* had larger bilateral bulges. The sister genera were marked different in structure, sequence and length (Fig. 22). The V3 helix showed the greatest deviation

Figs 1–15. Morphology of *Komarekiella delphini-convector* strain SJRDD-AB1 from cultured material. a, akinete; ag, akinete germination; vc, vegetative cell; mt, multiserial thallus; h, hormogonia; hf, formation of hormogonia; htc, heterocyte; tb, true branching. Scale bars = 10 μ m.

Fig. 1. Filamentous habit. Arrows indicate akinetes, vegetative cells and akinete germination.

Fig. 2. Pseudo-sarcinoid packets with a multiserial thallus.

Fig. 3. Another aspect of a multiserial thallus.

Fig. 4. Akinete germination.

Fig. 5. Filamentous growth with cell size differentiation.

Fig. 6. True branching.

Fig. 7. Cell differentiation in multiple planes.

Fig. 8. Akinete germination from a different growth state.

Fig. 9. Typical multiserial thallus from culture.

Fig. 10. Formation of hormogonia.

Fig. 11. Akinete development.

Fig. 12. Heterocyte larger than vegetative cell.

Fig. 13. Heterocyte of similar size as vegetative cell.

Fig. 14. Filamentous habit.

Fig. 15. Filamentous growth with heterocyte.

16

Subsystem Feature Counts

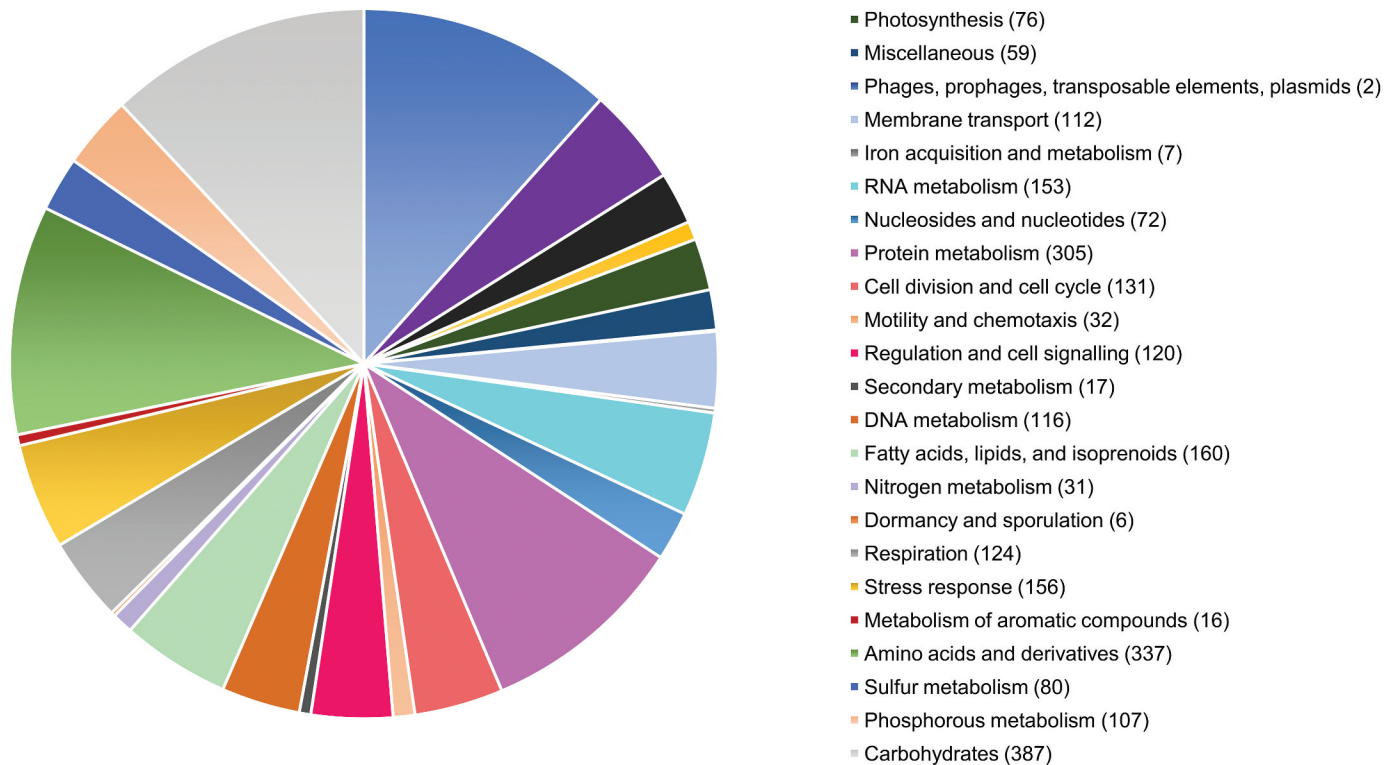


Fig. 16. A summary of subsystem functional categories derived from the whole genome of *Komarekiella delphini-convector*. The pie chart describes the count of each subsystem feature listed clockwise to the right.

in structure between the two species of *Komarekiella* (Fig. 23). The *K. delphini-convector* V3 helix was 83 nucleotides in length as compared to 54 nucleotides for *K. atlantica* (Table 1). There was one large insertion located within the internal portion of the helix, while the basal clamp and the basal bilateral bulge were highly conserved among the two species (Fig. 23). This insert facilitated several changes in the internal secondary structure of the stem. Additionally, a single nucleotide polymorphism was discovered in the terminal bulge for *K. delphini-convector* (Fig. 23). The V3 helices for the sister genera were again quite divergent from those of *Komarekiella* (Fig. 23).

Calculated ITS sequence p-distances showed *K. delphini-convector* strains were dissimilar to all *K. atlantica* strains, with p-distances ranging from 12.14 to 13.31. P-distances >7.00 are considered good evidence that two strains are separate species (Erwin & Thacker 2008; Osorio-Santos *et al.* 2014). Within-species dissimilarity for the two strains of *K. delphini-convector* was 0.17, while within-species dissimilarities among *K. atlantica* strains were 0.00–1.33 (Table 2), which are typical p-distances for within-species comparisons (Erwin & Thacker 2008; Osorio-Santos *et al.* 2014). The leader sequence in the ITS of *K. delphini-convector* was 1 nt longer than in *K. atlantica*. The spacer region between the D3 sequence and the tRNA^{Ile} gene was more than twice as long in *K. delphini-convector* than in *K. atlantica*, 25 nts compared to 12 nts. The spacer between the tRNA^{Ala} gene and

the Box B was 2 nts shorter in *K. delphini-convector*, while the spacers following the Box B and D4 domains had inserts 4 nt and 1 nt long, respectively, in *K. delphini-convector* compared to *K. atlantica* (Table 1). The final spacer sequence of the ITS for *K. delphini-convector* strain SJR- PJC1V1 was partial, ending 10 nts prior to the beginning of the 23S gene sequence, but did not vary in sequence from strain SJRDD-AB1 (Table 1).

Ribosomal strand secondary structure analyses

The secondary structure of the 16S rRNA molecule in *K. delphini-convector* was similar to that in *Nostoc commune* Bornet & Flahault (Řeháková *et al.* 2014), *Scytonema hyalinum* (Johansen *et al.* 2017) and *Aulosira bohemensis* Lukešová, J.R. Johansen, Michael P. Martin & Casamatta (Lukešová *et al.* 2009). It differed from all three by an insertion of a cytosine residue that forms a base-pair in the terminus of Helix 39, reducing the terminal loop from 6 nt to 5 nt (Fig. S2).

The secondary structure of the 23S rRNA molecule was very different from the structure reported for *Scytonema hyalinum* in helices 57–59 of Domain 3 (Johansen *et al.* 2017), with all three helices being longer in *K. delphini-convector* (Fig. S3). Domains 1–2 and 4–6 were identical to those found in *S. hyalinum* (Fig. S4; Johansen *et al.* 2017). The 5S rRNA structure was the same in *K. delphini-convector* as in *S. hyalinum* (Fig. S3). These two taxa are the only cyanobacteria for which secondary structures for the

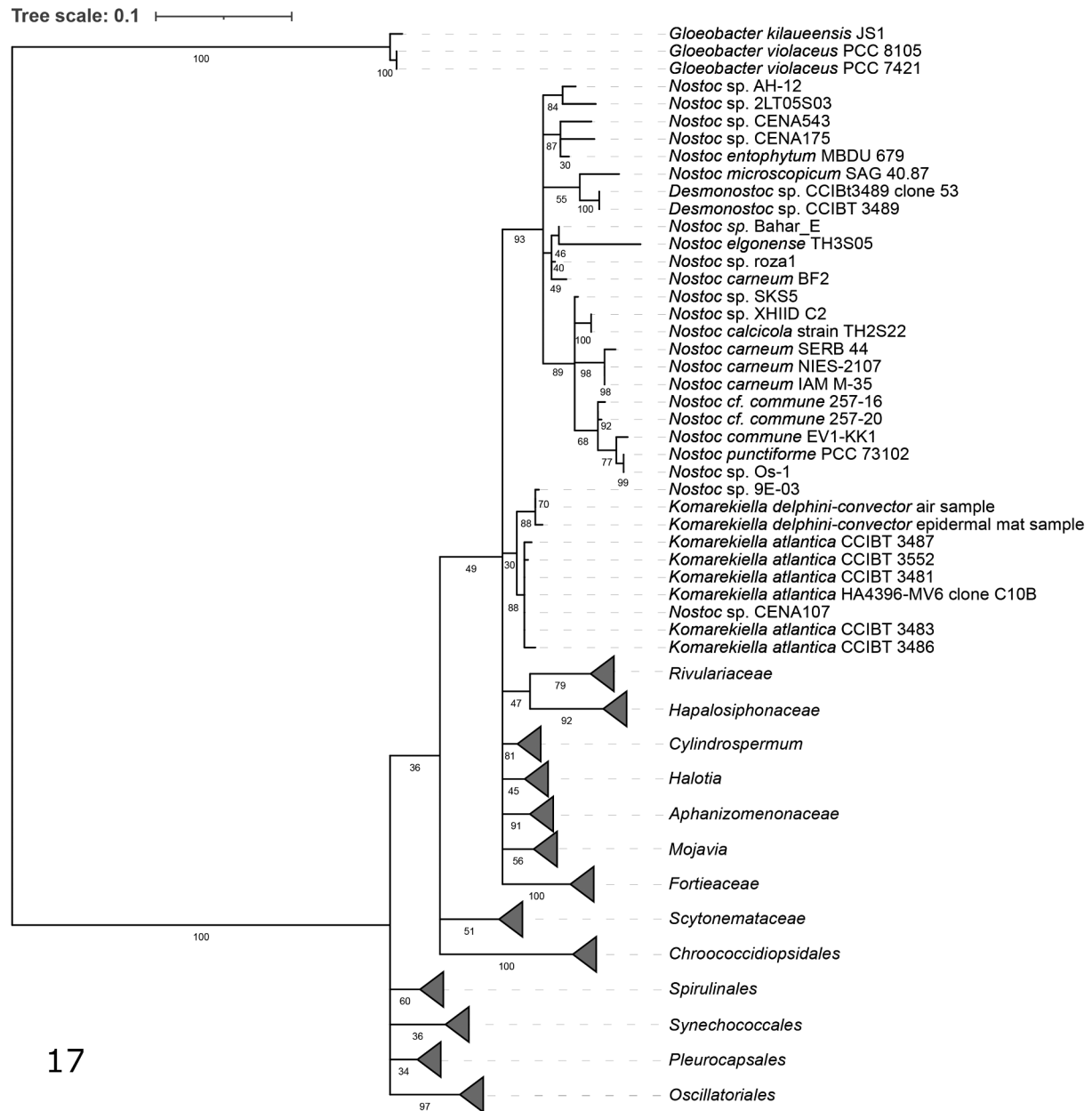


Fig. 17. Maximum Likelihood phylogeny based on the 16S rDNA sequences of 248 cyanobacterial strains with associated branch lengths and bootstrap support. *Gloebacter* sp. were used as outgroups.

23S rRNA molecule have been reported and suggest that differences in structure are likely to be found in more phylogenetically distant genera in other orders.

Toxin analyses: MCs/NODs (Adda ELISA and MMPB)

The Adda ELISA analysis for freely extracted MCs/NODs resulted in absorbances corresponding to concentrations just above the detection limits (1.5 and 3 ng g⁻¹). Toxin concentrations were 4.6, 5.0 and 4.5 ng g⁻¹ (wet weight) for the epidermal mat, BG-11 culture and Z-8 culture samples, respectively. However, MC-LR spike returns for extracted culture samples were low (≤6%), failing typical

quality control/assurance requirements for spike returns (70%–130%).

MMPB analysis of the oxidized ELISA extracts taken from culture samples did not support the ELISA results, as all extracts tested were below detection (<2.5 ng g⁻¹) for total Adda MCs/NODs. Total Adda MCs/NODs were also below detection (<1.3 ng g⁻¹) in oxidations of neat material (i.e. not previously extracted for ELISA analyses), further supporting that Adda MCs/NODs were not present in the samples. The MC-LR 20 ng g⁻¹ spikes conducted pre-extraction for ELISA were also below detection when extracts were oxidized and analysed for MMPB. In contrast, when culture samples were spiked directly, oxidized, extracted and analysed for MMPB, spike returns were 92% and 95%.

Tree scale: 0.1

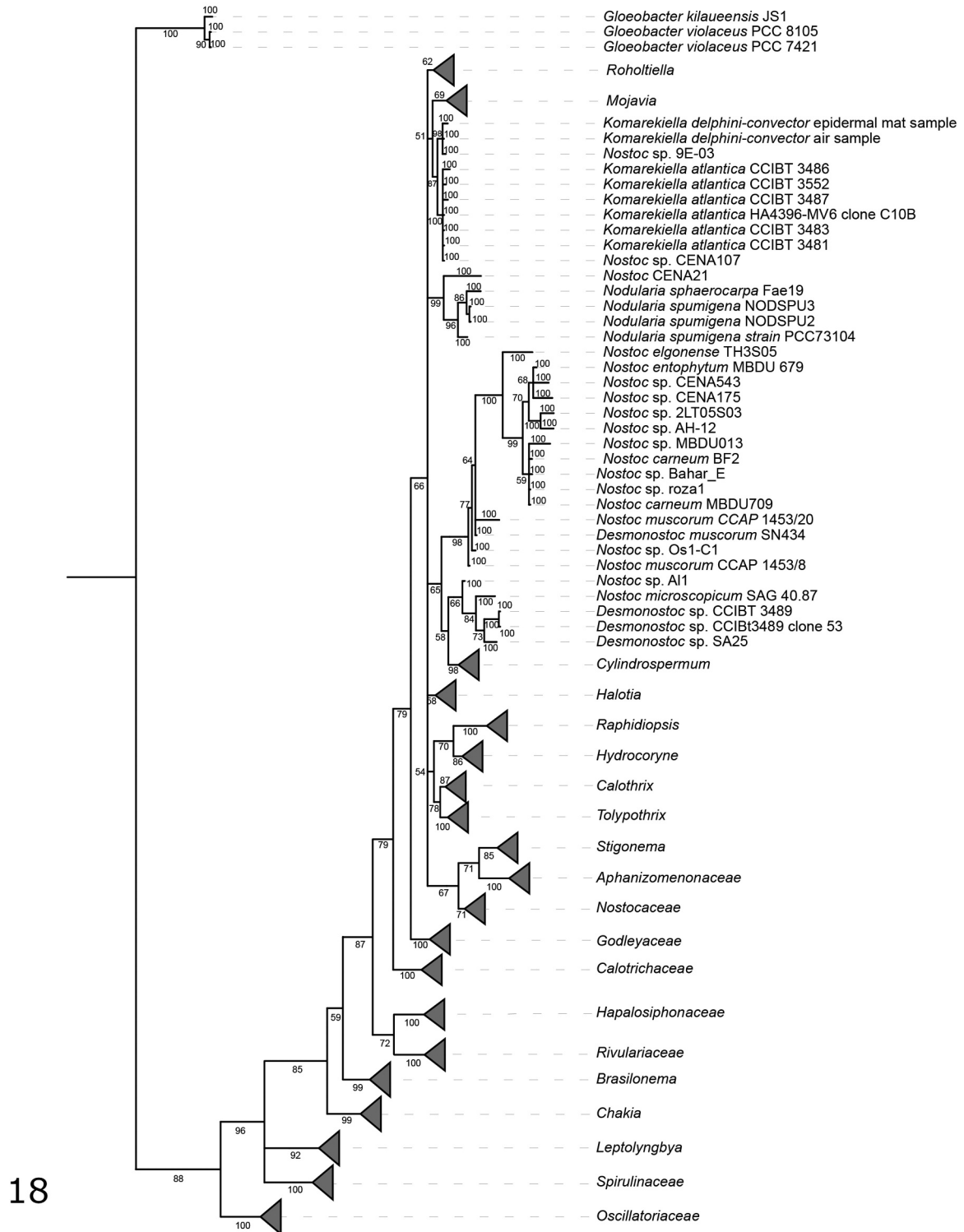


Fig. 18. Bayesian phylogeny based on 16S rDNA sequences of 248 cyanobacterial strains with associated branch lengths. *Gloeobacter* spp were used as outgroups.

Home range and core area

Kernel density analyses demonstrated that the home range of TtNEFL1501 prior to death included almost the entirety of the 40-km study area, including mesohaline (5–18 ppt) and oligohaline (0–3 ppt) areas of the SJR.

However, the dolphin's core area (50% UD) was located in mesohaline waters. TtNEFL1501 stranded approximately 44 km upriver from the furthest inland extent of the animal's documented home range in oligohaline water (Fig. S5).

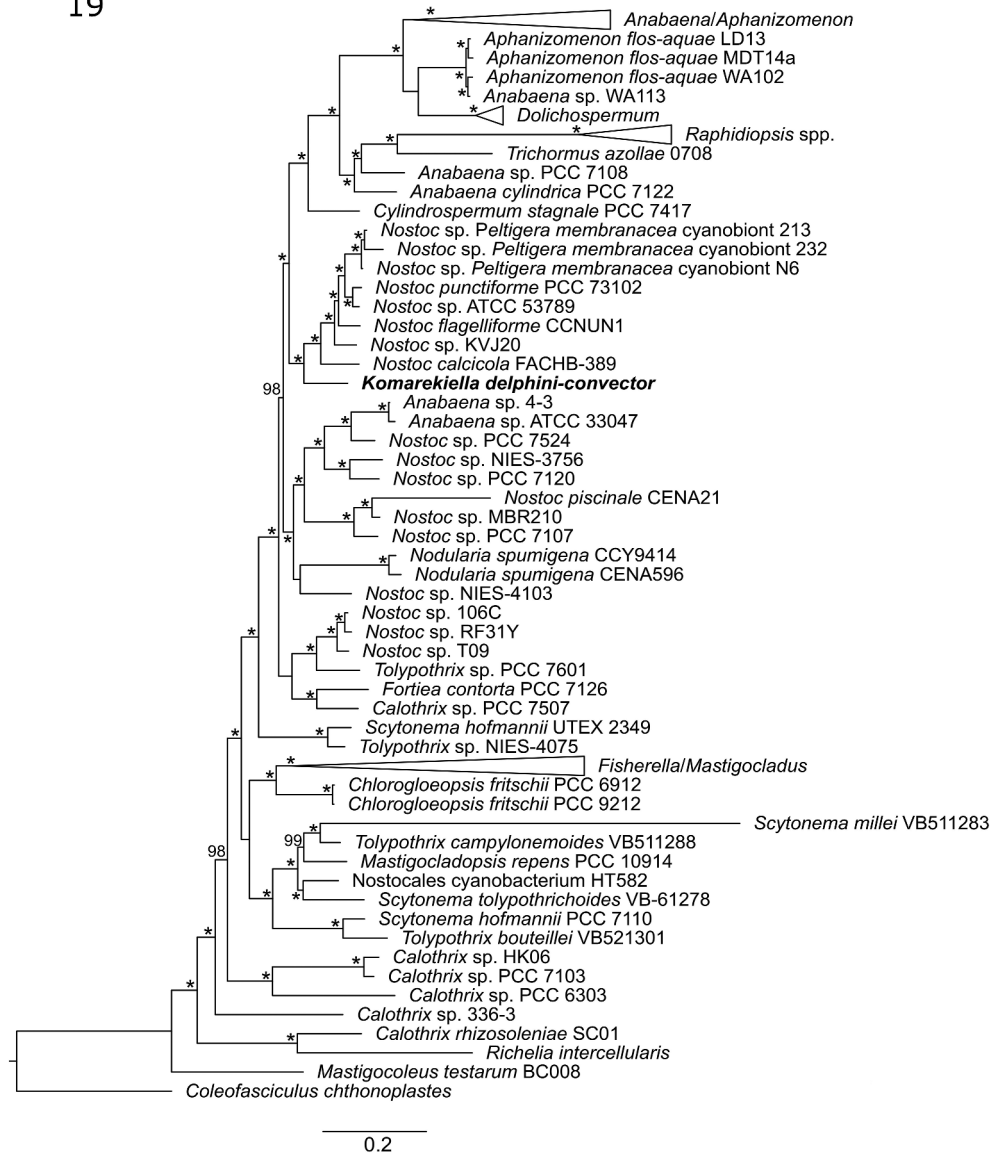


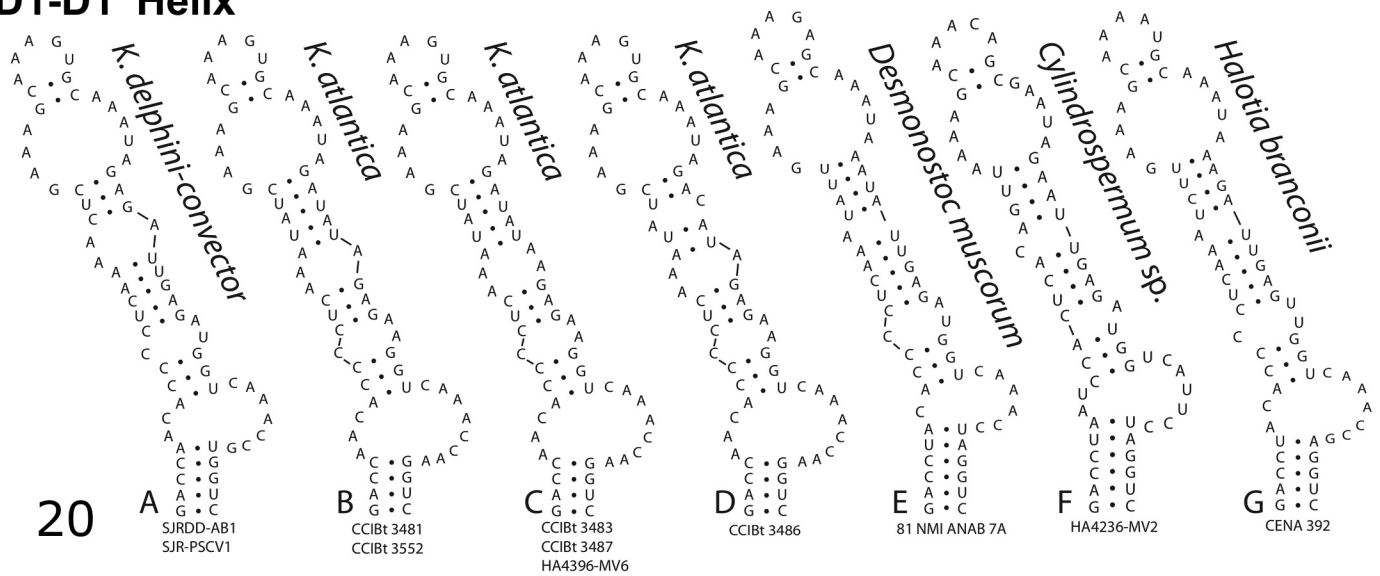
Fig. 19. A phylogenomic reconstruction of Nostocales cyanobacteria with *Coleofasciculus* as an outgroup based on 846 orthologous amino acid sequences. The studied strain is in bold. Asterisk represent 100% ultra-fast bootstrap support. Only bootstrap values above 98% are indicated.

DISCUSSION

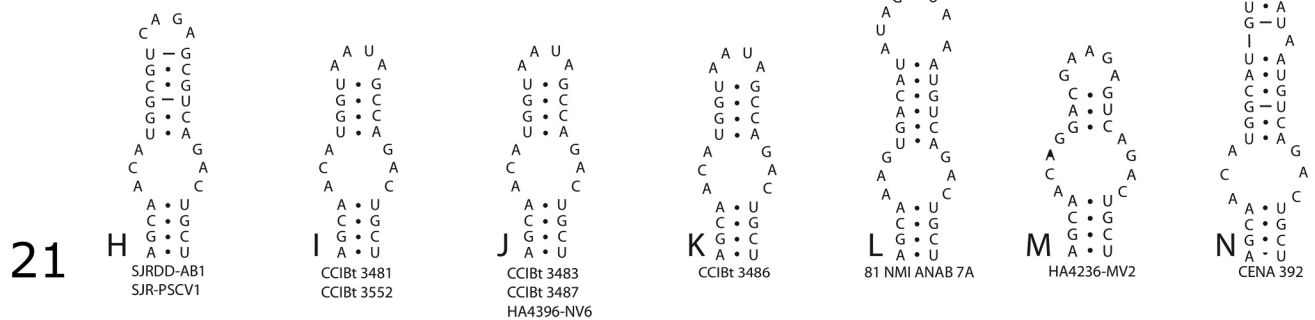
Results from a total evidence approach provide justification for the erection of a new taxon, *Komarekiella delphini-convector*, within the genus *Komarekiella*. The 16S rDNA phylogeny distinguished both *K. delphini-convector* strains as a distinctive node within the monophyletic *Komarekiella* taxa (the six *K. atlantica* strains). Phylogenomic analyses similarly separated *K. delphini-convector* from the *Nostoc sensu stricto* clade. Phylogenomic analyses also revealed multiple *Nostoc* clades that are distantly related to each other, supporting that *Nostoc* is polyphyletic and in need of revision. The phylogenetic variation within *Nostoc*, and its evident similarity to *Komarekiella*, has previously confounded efforts to classify isolates that are of close genetic and morphological resemblance. Originally isolated from epiphytes in subtropical and tropical trees of the Atlantic Rainforest, as well as from wet cement in Hawaii, it was suspected that *Komarekiella* was

a tropical genus of restricted distribution, for which environmental specificity would be a defining characteristic (Hentschke *et al.* 2017). This species may have also been misidentified as a species of *Nostoc* through 16S rDNA sequencing, as a part of an epilithic biofilm in a fountain in Granada, Spain (Cuzman *et al.* 2010). This research supports that *Komarekiella* is a more widespread taxon that may have been historically misidentified due to its rather remarkable phenotypic plasticity and resemblance to *Nostoc*. It is also noteworthy that occasional true branching was observed, which may complicate microscopic morphological identifications. Why *K. delphini-convector* exhibits true branching to the exclusion of its nearest neighbours remains an interesting question for further inquiry. Analyses of ITS indicated that there are two clades of *Komarekiella*, a tropical to equatorial clade and a subtropical to temperate clade, which are herein recognized as separate species. Distinct patterns of indels and mutations within the ITS, as well as variable secondary

D1-D1' Helix



Box-B Helix



Figs 20, 21. Secondary structures of the D1-D1', Box-B, V2 and V3 helices of *Komarekiella delphini-convector* and related taxa.

Fig. 20. D1-D1' helices of both *Komarekiella delphini-convector* strains compared to related taxa. The distinction between *K. delphini-convector* and *K. atlantica* helices is due to the constricted unilateral bulge and displacement of the internal bilateral bulge.

Fig. 21. Box-B helices of both *Komarekiella delphini-convector* strains in relation to related taxa. A 2-bp insert between the internal bilateral and terminal loop differentiates *K. delphini-convector* from *K. atlantica*.

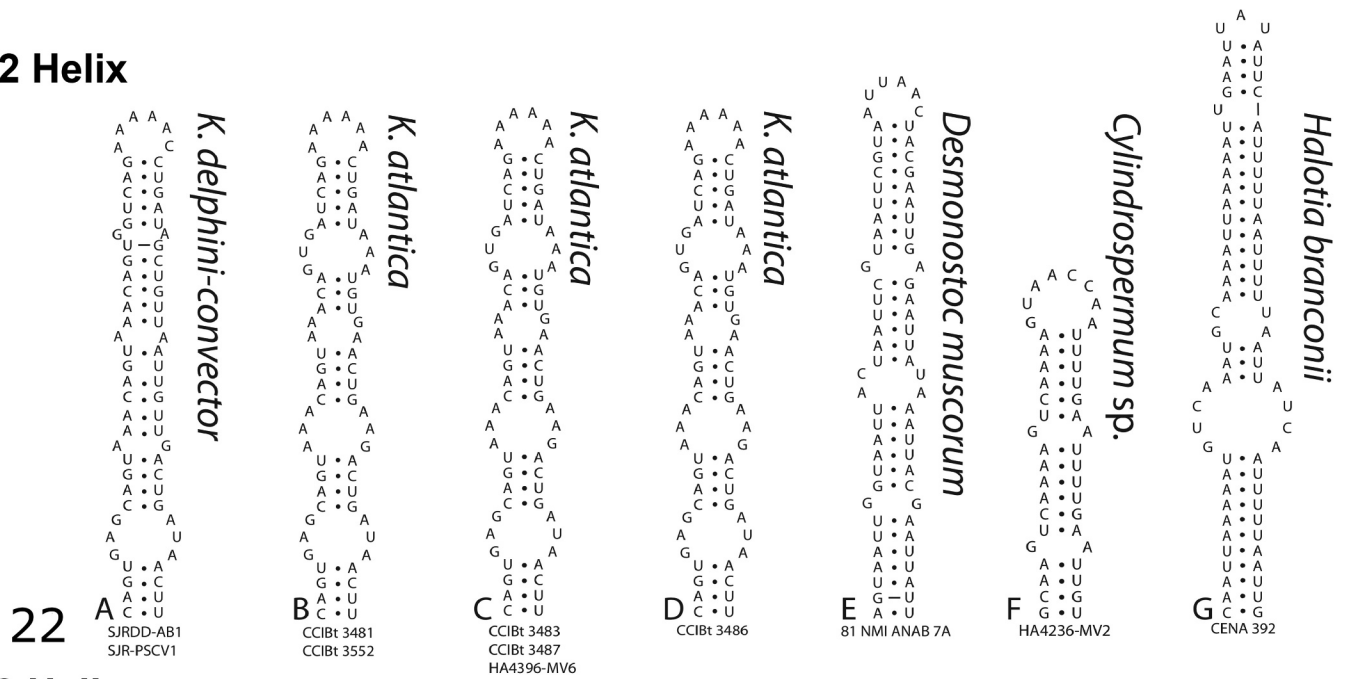
structures, clearly demonstrate evolutionary distance between the two species. Depending on the life history stage, this taxon could easily be mistaken for *Nostoc*, for taxa recently split from *Nostoc*, or for a number of colonial, coccoid cyanobacteria. Due to the stark similarities in ITS structures and sequences between *K. delphini-convector* strains and the phylogenetic separation from *K. atlantica*, it is likely that this species is endemic to the SJR, or at least that it has been isolated from the equatorial and tropical populations of *Komarekiella* that have been described previously. It bears noting that the recovery of one strain aerosolized above the St. Johns River may mean that the ability for long-distance dispersion is likely.

The presence of an epidermal mat on a bottlenose dolphin is unusual, as a dolphin's skin continuously sloughs off and is known to have microbial defence mechanisms against epiphytic colonization (Meyer & Seegers 2004). Epidermal growth is generally associated with freshwater exposure and poor skin condition (Barry *et al.* 2008, data from Lake Pontchartrain, Louisiana, USA; Mullin

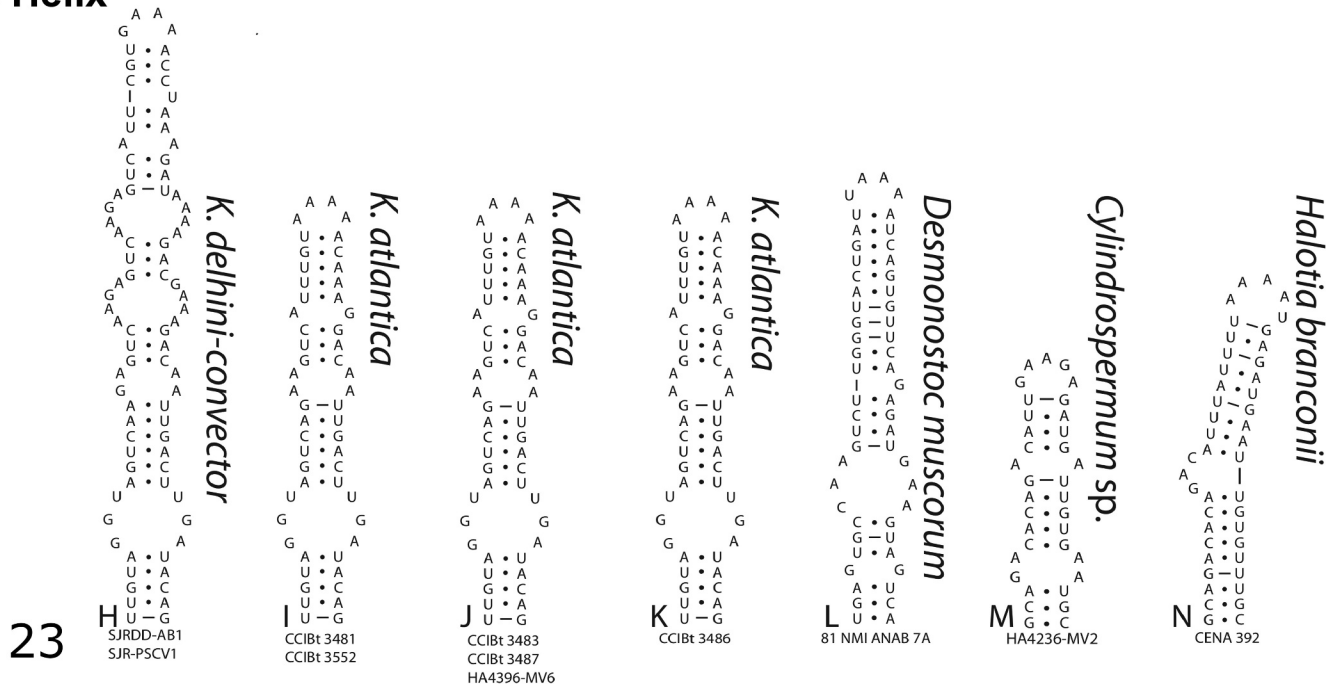
et al. 2015; W.N. Durden, unpublished data.; FWC, unpublished data). Supporting this, all three dolphins with epidermal mats in the SJR were described as 'out of habitat' and were recovered from low salinity waters (TtNEFL0813, 30°21.277'N, 81°36.697'W; TtNEFL1501, 30°1.745'N, 81°41.763'N; TtNEFL1511, 30°15.862'N, 81°41.869'W) (Fig. S6). Dolphins with epidermal growth associated with low salinity exposure have also been documented in other areas in the southeastern United States, including the Tomoka River and Bulow Creek in northeastern Florida (Ewing *et al.* 2017; Hubbs SeaWorld Research Institute, unpublished data; Fig. S6), and dolphins in the recent UME event in the Northern Gulf of Mexico (NOAA 2019).

TtNEFL1501 stranded 44 km upriver from the furthest inland extent of the dolphin's calculated home range (Fig. S5). Though the stranding location was described as unusual in relation to the habitat that the dolphin was consistently using, this could be an artefact due to the limitations of the 40 km survey route. The home range for TtNEFL1501, and other dolphins, may extend much further into low salinity

V2 Helix



V3 Helix



Figs 22, 23. Secondary structures of the D1-D1', Box-B, V2 and V3 helices of *Komarekiella delphini-convector* and related taxa.

Fig. 22. V2 helices from both *Komarekiella delphini-convector* strains in relation to other taxa. *K. delphini-convector* is distinguished from *K. atlantica* by smaller bilateral bulges.

Fig. 23. V3 helices of both of the *Komarekiella delphini-convector* strains compared to other closely related taxa. Marked differences are seen in nucleotide length between *K. delphini-convector* and *K. atlantica*.

habitats, which are not routinely surveyed. Interestingly, records of non-specific epidermal 'algal' growth have also been reported in free-swimming and stranded dolphins within the Indian River Lagoon. In one instance, histological evidence demonstrated that the algal growth penetrated the muscle tissue (W.N. Durden, unpublished data). However, this algal growth extending through the tissue layers of the animal could have been associated with opportunistic colonization in a deep, open wound caused by a vessel strike (W.N.

Durden, unpublished data). Further research is needed to evaluate the conditions under which algal growth is facilitated as well as the potential health impacts on dolphin populations.

Komarekiella delphini-convector may not be a direct pathogen but could have been facilitated by the infection of other microbes present in the epidermal consortia, which were not determined in this study. No histologic data was taken for TtNEFL1501 and thus it was not confirmed whether this species bored into the epidermis pre- or post-mortem.

Table 1. Comparison of lengths in numbers of nucleotides of conserved and spacer ITS domains for *Komarekiella delphini-convector* strains (A, SJRDD-AB1; B, SJR-PJCV1) and strains of the sister species *Komarekiella atlantica*.

Strain	Leader	D1-D1' Helix	spacer+D2 + spacer	D3 + spacer	tRNA Ile gene	spacer+V2 + spacer	tRNA		Box-B + spacer	Box A	D4 + spacer	V3+ ITS end (*partial)
							Ala gene	Spacer				
<i>K. delphini-convector</i> strain A	8	65	39	25	74	82	73	39	47	11	21	100
<i>K. delphini-convector</i> strain B	8	65	39	25	74	82	73	39	47	11	21	91*
<i>K. atlantica</i> CCIBT 3483	7	66	39	12	74	82	73	41	43	11	20	71
<i>K. atlantica</i> CCIBT 3481	7	65	39	12	74	82	73	41	43	11	20	71
<i>K. atlantica</i> CCIBT 3487	7	66	39	12	74	82	73	41	43	11	20	71
<i>K. atlantica</i> CCIBT 3552	7	65	39	12	74	82	73	41	43	11	20	71
<i>K. atlantica</i> CCIBT 3486	7	65	39	12	74	82	73	41	43	11	20	71
<i>K. atlantica</i> HA4396-MV6 clone C10B	7	65	39	12	74	82	73	41	43	11	20	71
<i>K. atlantica</i> HA4396-MV6 clone C10A	7	65	39	12	74	82	73	41	43	11	20	71

Table 2. Calculated p-distances expressed as percent dissimilarities for ITS sequences of both *Komarekiella delphini-convector* strains (A, SJRDD-AB1; B, SJR-PJCV1) and four *Komarekiella atlantica* strains. Indels were included in the calculations, but the final 10 nucleotides prior to the 23S gene were discarded due to the incomplete sequence of *Komarekiella delphini-convector* strain SJR-PJCV1.

<i>K. delphini-convector</i> strain A												
<i>K. delphini-convector</i> strain B			0.17									
<i>K. atlantica</i> CCIBT 3483 (KX638487.1)			12.71	12.52								
<i>K. atlantica</i> CCIBT 3481 (KX638484.1)			13.31	13.12	1.33							
<i>K. atlantica</i> CCIBT 3487 (KX638488.1)			12.74	12.55	1.14	0.57						
<i>K. atlantica</i> CCIBT 3552 (KX638485.1)			13.31	13.12	1.33	0.57	0.38					
<i>K. atlantica</i> CCIBT 3486 (KX638489.1)			12.33	12.14	0.57	1.13	0.95	1.13				
<i>K. atlantica</i> HA4396-MV6 clone C10B (KX646832.1)			12.33	12.14	0.57	1.13	0.95	1.13	0.00			

Regardless, it is possible that *K. delphini-convector* has boring capabilities based on its growth in culture and the necropsy photos and descriptions. Certain cyanobacterial species have boring capabilities and have been previously implicated as causative agents of epidermal disease (e.g. in manatees; Harr *et al.* 2008) or as facilitators of opportunistic infections by providing an entry through the epidermis (e.g. in coral black band disease; Miller *et al.* 2011).

Extensive genome mining using numerous secondary metabolite prediction tools revealed that this species has a plethora of biosynthetic gene clusters for the potential production of bioactive compounds. Initial genome annotation using RAST identified 8,439 coding sequences, of which 13 features were identified as belonging to secondary metabolism. These features pertained to UV-absorbing metabolites and the production of plant hormones, such as auxin. Secondary metabolite biosynthetic gene clusters (smBGCs) were identified using NaPDoS, antiSMASH, BAGEL4 and PRISM. NaPDoS indicated the presence of 18 KS domains and 30 C domains, antiSMASH predicted 24 smBGCs, PRISM predicted 16 smBGCs, while BAGEL4 identified 4 smBGCs. Of the 92-total predicted smBGCs, 16 were detected at the same genomic locus by the different bioinformatics tools.

The microcystin/nodularin (MC/NOD) producing capability of *K. delphini-convector* was not conclusively determined based on findings derived from Adda ELISA, MMPB, and full genome mining. The Adda ELISA analysis of extracted dermal mat and cultured material resulted in positive detections of MCs/NODs (4.5–5.0 ng g⁻¹). However, this observation was not supported by the MMPB technique, where all samples

were below detection (<2.5 ng g⁻¹) for total Adda MCs/NODs. This supports that the Adda ELISA used in this work was responding to matrix (non-specific binding with kit antibodies) and provided false positive data, which has also been observed in other work (Brown *et al.* 2018; Foss *et al.* 2019). It was determined that the extractant solution used in this work (75% MeOH/100 mM acetic acid) was not suitable for recovering MCs/NODs from agar, as supported by the near complete MC-LR spike loss (observed in both Adda ELISA and MMPB analyses). In contrast, it was determined that agar can be oxidized and allow for the release of the MMPB molecule for analysis by LC-MS/MS, as evidenced by the MC-LR pre-oxidation spike recoveries (92%–95%). Therefore, this limited work illustrates the need to further investigate extraction methods suitable for the analysis of intact MCs/NODs from agar cultures.

This work identified a new species of a cryptic and epizoic cyanobacteria through morphologic and genetic analyses. The natural history of the genus *Komarekiella* was also expanded through additional reports as an epizoic and in a bioaerosol. The observational and limited results from current genome mining and toxin analysis prevented any conclusion about toxin producing capabilities. However, these research gaps warrant further investigation into the pathogenic and toxigenic capabilities of epizoic cyanobacteria.

ACKNOWLEDGEMENTS












The authors thank Mark Aubel, Sarah Fuller and Kamil Cieslik for laboratory assistance in toxin analyses and methodology. We extend

thanks to the Coastal Biology Flagship Program and the Environmental Center (University of North Florida) for funding. We thank Florida Fish and Wildlife Conservation Commission North East Field lab, Nadia Gordon, Allison Perna, and volunteers for their time and effort in sample collection and providing all available information for TtNEFL0813, TtNEFL1501 and TtNEFL1511. All photo-identification data were collected under authorization of NOAA Fisheries GA LOC 14157, 20377-01 and Permit 18182, as well as UNF's IACUC (approval #11-003 and #13-006). The authors have no conflicts of interest to declare.

FUNDING

This project was funded by the Internal Grant Agency of the Palacký University - Prf-2021-001, the University of North Florida Institute of Environmental Research and Education, the University of North Florida Department of Biology and UNF Coastal Biology Flagship Program.

ORCID

Amber O. Brown  <http://orcid.org/0000-0002-6761-2170>
 Caitlin S. Romanis  <http://orcid.org/0000-0001-5036-6922>
 Petr Dvořák  <http://orcid.org/0000-0003-0101-9566>
 Amanda J. Foss  <http://orcid.org/0000-0003-0412-3879>
 Quincy A. Gibson  <http://orcid.org/0000-0003-0043-774X>
 Chelsea D. Villanueva  <http://orcid.org/0000-0002-8969-5747>
 Wendy N. Durden  <http://orcid.org/0000-0002-5095-4334>
 Petr Hašler  <http://orcid.org/0000-0003-4658-1114>
 Jeffrey R. Johansen  <http://orcid.org/0000-0002-0794-9417>
 Brett A. Neilan  <http://orcid.org/0000-0001-6113-772X>
 Dale A. Casamatta  <http://orcid.org/0000-0002-8056-0715>

REFERENCES

- Allen M.M. & Stanier R.Y. 1968. Growth and division of some unicellular blue-green algae. *Journal of General Microbiology* 51: 199–202. DOI:10.1099/00221287-51-2-199.
- Andersen R.A. 2005. *Algal culturing techniques*. Elsevier Academic Press New York, New York, USA. 578 pp.
- Aziz R.K., Bartels D., Best A.A., DeJongh M., Disz T., Edwards R.A., Formsma K., Gerdes S., Glass E.M., Kubal M. et al. 2008. The RAST server: rapid annotations using subsystems technology. *BMC Genomics* 9: Article 75. DOI:10.1186/1471-2164-9-75.
- Bankevich A., Nurk S., Antipov D., Gurevich A.A., Dvorkin M., Kulikov A.S., Lesin V.M., Nikolenko S.I., Pham S., Pribelski A.D. et al. 2012. SPAdes: a new genome assembly algorithm and its applications to single-cell sequencing. *Journal of Computational Biology* 19: 455–477. DOI: 10.1089/cmb.2012.0021.
- Barry K.P., Gorgone A.M. & Mase B. 2008. *Lake Pontchartrain, Louisiana bottlenose dolphin survey summary 28 April 2008–10 May 2008*. Southeast Fisheries Science Center, National Marine Fisheries Service, NOAA Protected Resources and Biodiversity Division, PRBD Contribution: PRBD-08/09-01.
- Blin K., Shaw S., Steinke K., Villebro R., Ziemert N., Lee S.Y., Medema M.H. & Weber T. 2019. antiSMASH 5.9: updates to the secondary metabolite genome mining pipeline. *Nucleic Acids Research* 47: 81–87. DOI:10.1093/nar/gkz310.
- Bolger A.M., Lohse M. & Usadel B. 2014. Trimmomatic: a flexible trimmer for Illumina sequence data. *Bioinformatics* 30: 2114–2120. DOI:10.1093/bioinformatics/btu170.
- Bornet É. & Flahault C. 1886. ('1888'). Revision des Nostocacées hétérocystées contenues dans les principaux herbiers de France (quatrième et dernier fragment). *Annales des Sciences Naturelles, Botanique, septième série* 7: 177–262.
- Boyer S.L., Flechtner V.R. & Johansen J.R. 2001. Is the 16S-23S rRNA Internal Transcribed Spacer region a good tool for use in molecular systematics and population genetics? A case study in cyanobacteria. *Molecular Biology and Evolution* 18: 1057–1069. DOI:10.1093/oxfordjournals.molbev.a003877.
- Brown A.O., Foss A.J., Miller M.A. & Gibson Q.G. 2018. Detection of cyanotoxins (microcystins/nodularins) in livers from estuarine and coastal bottlenose dolphins (*Tursiops truncatus*) from Northeast Florida. *Harmful Algae* 76: 22–34. DOI:10.1016/j.hal.2018.04.011.
- Caldwell M. 2001. *Social and genetic structure of bottlenose dolphin (Tursiops truncatus) in Jacksonville, Florida*. PhD thesis. University of Miami. 143 pp.
- Carmichael R.H., Graham W.M., Aven A., Worthy G. & Howden S. 2012. Were multiple stressors a “perfect storm” for Northern Gulf of Mexico bottlenose dolphins (*Tursiops truncatus*) in 2011? *PLOS One* 7: Article e41155. DOI:10.1371/journal.pone.0041155.
- Casamatta D.A., Vis M.L. & Sheath R.G. 2003. Cryptic species in cyanobacterial systematics: a case study of *Phormidium retzii* (Oscillatoriales) using 16S rDNA and RAPD analyses. *Aquatic Botany* 77: 295–309. DOI:10.1016/j.aquabot.2003.08.005.
- Castresana J. 2000. Selection of conserved blocks from multiple alignments for their use in phylogenetic analysis. *Molecular Biology and Evolution* 17: 540–552. DOI:10.1093/oxfordjournals.molbev.a026334.
- Christiansen G., Molitor C., Philmus B. & Kurmayer R. 2008. Nontoxic strains of cyanobacteria are the result of major gene deletion events induced by a transposable element. *Molecular Biology and Evolution* 8: 1695–1704. DOI:10.1093/molbev/msn120.
- Cuzman O.A., Ventura S., Sili C., Mascacchi C., Turchetti T., D'Acqui L. P. & Tianio P. 2010. Biodiversity of phototrophic biofilms dwelling on monumental fountains. *Microbial Ecology* 60: 81–95. DOI:10.1007/s00248-010-9672-z.
- Darriba D., Taboada G.L., Doallo R. & Posada D. 2012. jModelTest 2: more models, new heuristics and high-performance computing. *Nature Methods* 9: 772. DOI:10.1038/nmeth.2109.
- Davis D.A., Mondo K., Stern E., Annor A.K., Murch S.J., Coyne T.M., Brand L.E., Niemeyer M.E., Sharp S., Bradley W.G. et al. 2019. Cyanobacterial neurotoxin BMAA and brain pathology in stranded dolphins. *PLOS One* 14: Article 3. DOI:10.1371/journal.pone.0213346.
- Douterelo I., Perona E. & Mateo P. 2004. Use of cyanobacteria to assess water quality in running waters. *Environmental Pollution* 127: 377–384. DOI:10.1016/j.envpol.2003.08.016.
- Dvořák P., Casamatta D.A., Hašler P., Ondřej V., Pouličková A. & Sanges R. 2014. *Synechococcus*: 3 billion years of global dominance. *Molecular Ecology* 23: 5538–5551. DOI:10.1111/mec.12948.
- Edgar R.C. 2004. MUSCLE: multiple sequence alignment with high accuracy and high throughput. *Nucleic Acids Research* 32: 1792–1797. DOI:10.1093/nar/gkh340.
- Environmental Protection Board, City of Jacksonville. 2017. *River report. State of the lower St. Johns River basin, Florida: water quality, fisheries, aquatic life, contaminants, 2017*. State of the River Report. 8 pp.
- Ermak J., Karle K. & Gibson Q. 2017. Multi-level dolphin alliances in northeastern Florida offer comparative insight into pressures shaping alliance formation. *Journal of Mammalogy* 98: 1096–1104. DOI:10.1093/jmammal/gyx053.
- Erwin P.M. & Thacker R.W. 2008. Cryptic diversity of the symbiotic cyanobacterium *Synechococcus spongiarum* among sponge hosts. *Molecular Ecology* 12: 2937–2947. DOI:10.1111/j.1365-294X.2008.03808.x.
- Ewing R.Y., Mase-Guthrie B., McFee W., Townsend F., Manire C.A., Walsh M., Borkowski R., Bossart G.D. & Schaefer A.M. 2017. Evaluation of serum for pathophysiological effects of prolonged low salinity water exposure in displaced bottlenose dolphins (*Tursiops truncatus*). *Frontiers in Veterinary Science* 4: Article 80. DOI:10.3389/fvets.2017.00080.
- Foss A.J., Butt J., Fuller S., Cieslik K., Aubel M.T. & Wertz T. 2017. Nodularin from benthic freshwater periphyton and implications for trophic transfer. *Toxicon* 140: 45–59. DOI:10.1016/j.toxicon.2017.10.023.
- Foss A.J., Aubel M.T., Gallagher B., Mettee N., Miller A. & Fogelson S.B. 2019. Diagnosing microcystin intoxication of canines: clinicopathological indications, pathological characteristics, and analytical detection in postmortem and antemortem samples. *Toxins* 11: Article 456. DOI:10.3390/toxins11080456.

- Furtado A.L.F.F., Do Carmo Calijuri M., Lorenzi A.S., Honda R.Y., Genuário D.B. & Fiore M.F. 2009. Morphological and molecular characterization of cyanobacteria from a Brazilian facultative wastewater stabilization pond and evaluation of microcystin production. *Hydrobiologia* 627: 195–209. DOI:10.1007/s10750-009-9728-6.
- Gubbins C. 2002. Use of home ranges by resident bottlenose dolphins (*Tursiops truncatus*) in a South Carolina estuary. *Journal of Mammalogy* 83: 178–187. DOI:10.1644/1545-1542(2002)083<0178:UOHRBR>2.0.CO;2.
- Harr K.E., Szabo N.J., Cichra M. & Philps E.J. 2008. Debruoaplysiatoxin in *Lyngbya*-dominated mats on manatees (*Trichechus manatus latirostris*) in the Florida King's Bay ecosystem. *Toxicol* 52: 385–388. DOI:10.1016/j.toxicol.2008.05.016.
- Hentschke G.S., Johansen J.R., Pietrasiak N., Rigonato J., Fiore M.F. & Sant'anna C.L. 2017. *Komarekiella atlantica* gen. et sp. nov. (Nostocaceae, Cyanobacteria): a new subaerial taxon from the Atlantic Rainforest and Kauai, Hawaii. *Fottea* 17: 178–190. DOI:10.5507/fot.2017.002.
- Iteman I., Rippka R., Tandeau De Marsac N. & Herdman M. 2000. Comparison of conserved structural and regulatory domains within divergent 16S rRNA-23S rRNA spacer sequences of cyanobacteria. *Microbiology* 146: 1275–1286. DOI:10.1099/00221287-146-6-1275.
- Johansen J.R. & Casamatta D.A. 2005. Recognizing cyanobacterial diversity through adoption of a new species paradigm. *Algological Studies* 117: 71–93.
- Johansen J.R., Mareš J., Pietrasiak N., Bohunická M., Zima J., Jr., Štenclová L. & Hauer T. 2017. Highly divergent 16S rRNA sequences in ribosomal operons of *Scytonema hyalinum* (Cyanobacteria). *PLOS One* 12: Article e0186393.
- Komárek J. 2003. Problem of the taxonomic category “species” in cyanobacteria. *Algological Studies* 109: 281–297.
- Komárek J. 2010. Recent changes (2008) in cyanobacteria taxonomy based on a combination of molecular background with phenotype and ecological consequences (genus and species concept). *Hydrobiologia* 639: 245–259. DOI:10.1007/s10750-009-0031-3.
- Komárek J., Kaštovský J., Mareš J. & Johansen J.R. 2014. Taxonomic classification of cyanoprokaryotes (cyanobacterial genera) 2014 using a polyphasic approach. *Preslia* 86: 295–335.
- Laamanen M.J., Gugger M.F., Lehtimäki J.M., Haukka K. & Sivonen K. 2001. Diversity of toxic and nontoxic *Nodularia* isolates (cyanobacteria) and filaments from the Baltic Sea. *Applied and Environmental Microbiology* 67: 4638–4647. DOI:10.1128/AEM.67.10.4638-4647.2001.
- Lagesen K., Hallin P., Rødland E.A., Staerfeldt H.H., Rognes T. & Ussery D.W. 2007. RNAmmer: consistent and rapid annotation of ribosomal RNA genes. *Nucleic Acids Research* 35: 3100–3108. DOI:10.1093/nar/gkm160.
- Lane D.J. 1991. 16S/23S rRNA sequencing. In: *Nucleic acid techniques in bacterial systematics* (Ed. by E. Stackebrandt & M. Goodfellow), pp 115–175. John Wiley and Sons, New York, New York, USA.
- Letunic I. & Bork P. 2019. Interactive Tree of Life (iTOL) v4: recent updates and new developments. *Nucleic Acids Research* 47: W256–W259. DOI:10.1093/nar/gkz239.
- Lukešová A., Johansen J.R., Martin M.P. & Casamatta D.A. 2009. *Aulosira bohemensis* sp. nov.: further phylogenetic uncertainty at the base of the Nostocales (Cyanobacteria). *Phycologia* 48: 118–129. DOI:10.2216/08-56.1.
- Meyer W. & Seegers U. 2004. A preliminary approach to epidermal antimicrobial defence in the Delphinidae. *Marine Biology* 144: 841–844. DOI:10.1007/s00227-003-1256-8.
- Miller A.W., Blackwelder P., Al-Sayegh H. & Richardson L.L. 2011. Fine-structural analysis of black band disease-infected coral reveals boring cyanobacteria and novel bacteria. *Diseases of Aquatic Organisms* 93: 179–190. DOI:10.3354/dao02305.
- Montagu G. 1821. Description of a species of *Delphinus*, which appears to be new. *Memoirs of the Wernerian Natural History Society* 3: 75–82.
- Mullin K.D., Barry K., Sinclair C., Litz J., Maze-Foley K., Fougères E., Mase-Guthrie B., Weing R., Gorgone A., Adams J. et al. 2015. *Common bottlenose dolphins (Tursiops truncatus) in Lake Pontchartrain, Louisiana: 2007 to mid-2014*. NOAA Technical Memorandum NMFS-SEFSC-673. 43 pp.
- Nguyen L.T., Schmidt H.A., von Haeseler A. & Minh B.Q. 2015. IQ-TREE: a fast and effective stochastic algorithm for estimating Maximum-Likelihood phylogenies. *Molecular Biology and Evolution* 32: 268–274. DOI:10.1093/molbev/msu300.
- NOAA – National Oceanic and Atmospheric Administration. 2019. 2019 Bottlenose dolphin unusual mortality event along the Northern Gulf of Mexico. <https://www.fisheries.noaa.gov/national/marine-life-distress/2019-bottlenose-dolphin-unusual-mortality-event-along-northern-gulf>; searched on December 19, 2019.
- Osorio-Santos K., Pietrasiak N., Bohunická M., Miscoe L.H., Kováčik L., Martin M.P. & Johansen J.R. 2014. Seven new species of *Oculatella* (Pseudanabaenales, Cyanobacteria): taxonomically recognizing cryptic diversification. *European Journal of Phycology* 49: 450–470. DOI:10.1080/09670262.2014.976843.
- Otsuka S., Suda S., Li R.H., Watanabe M., Oyaizu H., Matsumoto S. & Watanabe M.M. 1999. Phylogenetic relationships between toxic and nontoxic strains of the genus *Microcystis* based on 16S to 23S internal transcribed spacer sequence. *FEMS Microbiology Letters* 172: 15–21. DOI:10.1111/j.1574-6968.1999.tb13443.x.
- Řeháková K., Johansen J.R., Bowen M.B., Martin M.P. & Sheil C.A. 2014. Variation in secondary structure of the 16S rRNA molecule in cyanobacteria with implications for phylogenetic analysis. *Fottea* 14: 161–178. DOI:10.5507/fot.2014.013.
- Robbette B., Yoder R.J., Boyd A., Reeves J. & Spatafora J.W. 2011. Hal: an automated pipeline for phylogenetic analyses of genomic data. *PLoS Currents* 3: Article RRN1213. DOI:10.1371/currents.RRN1213.
- Ronquist F., Teslenko M., Van Der Mark P., Ayres D.L., Darling A., Höhna S., Lieret B., Liu L., Suchard M.A. & Huelsenbeck J.P. 2012. MrBayes 3.2: efficient Bayesian phylogenetic inference and model choice across a large model space. *Systematic Biology* 61: 539–542. DOI:10.1093/sysbio/sys029.
- Skinninger M.A., Dejong C.A., Rees P.N., Johnston C.W., Li H., Webster A.L.H., Wyatt M.A. & Magarvey N.A. 2015. Genomes to natural products Prediction Informatics for Secondary Metabolites (PRISM). *Nucleic Acids Research* 42: 9645–9662.
- Stamatakis A. 2003. RAXML version 8: a tool for phylogenetic analysis and post-analysis of large phylogenies. *Bioinformatics* 30: 1312–1313. DOI:10.1093/bioinformatics/btu033.
- Staub R. 1961. Ernährungsphysiologisch-autökologische Untersuchungen an der planktischen Blaualge *Oscillatoria rubescens* DC. *Schweizerische Zeitschrift für Hydrologie* 23: 82–198.
- Turland N.J., Wiersema J.H., Barrie F.R., Greuter W., Hawksworth D.L., Herendeen P.S., Knapp S., Kusber W.-H., Li D.-Z., Marhold K. et al. [Eds]. 2018. *International Code of Nomenclature for algae, fungi, and plants (Shenzhen Code) adopted by the Nineteenth International Botanical Congress Shenzhen, China, July 2017*. Koeltz Botanical Books, Glashütten, Germany. xxxviii + 254 pp. [Regnum Vegetabile 159]. DOI:10.12705/Code.2018.
- Van Heel A.J., de Jong A., Song C., Viel J.H., Kok J. & Kuipers O.P. 2018. BAGEL4: a user-friendly web server to thoroughly mine RiPPs and bacteriocins. *Nucleic Acids Research* 46: W278–W281. DOI:10.1093/nar/gky383.
- Wehr J.D., Sheath R.G. & Kociolek J.P. [Eds]. 2015. *Freshwater algae of North America: ecology and classification*, ed. 2. Academic Press, San Diego, California, USA. 1066 pp.
- Wilson B., Arnold H., Bearzi G., Fortuna C., Gaspar R., Ingram S., Liret C., Pribanic A.J., Read J., Ridoux V. et al. 1999. Epidermal diseases in bottlenose dolphins: impacts of natural and anthropogenic factors. *Proceedings of the Royal Society of London, Biology* 266: 1077–1083. DOI: 10.1098/rspb.1999.0746.
- Wu Y., Simmons W. & Singer S.W. 2016. MaxBin 2.0: an automated binning algorithm to recover genomes from multiple metagenomic datasets. *Bioinformatics* 32: 605–607. DOI:10.1093/bioinformatics/btv638.
- Ziemert N., Podell S., Penn K., Badger J.H., Allen E. & Jensen P.R. 2012. The Natural Product Domain Seeker NaPDoS: a phylogeny based bioinformatic tool to classify secondary metabolite gene diversity. *PLOS One* 7: Article e34064. DOI:10.1371/journal.pone.0034064.
- Zuker M. 2003. Mfold web server for nucleic acid folding and hybridization prediction. *Nucleic Acids Research* 31: 3406–3415. DOI: 10.1093/nar/gkg595.